ACADEMIC PRESS

Available online at www.sciencedirect.com

SCIENCE DIRECT®

Toxicology and Applied Pharmacology 190 (2003) 157–169

Toxicology and Applied Pharmacology

www.elsevier.com/locate/taap

Oxidative stress and NFκB activation in the lungs of rats: a synergistic interaction between soot and iron particles

Ya-Mei Zhou,[a] Cai-Yun Zhong,[a] Ian M. Kennedy,[b] Valerie J. Leppert,[c] and Kent E. Pinkerton[a,*]

[a] *Center for Health and the Environment, Department of Anatomy, Physiology, and Cell Biology, School of Veterinary Medicine, University of California, Davis, CA 95616, USA*

[b] *Department of Mechanical and Aeronautical Engineering, University of California, Davis, CA 95616, USA*

[c] *Department of Chemical Engineering and Materials Science, College of Engineering, University of California, Davis, CA 95616, USA*

Received 30 September 2002; accepted 4 March 2003

Abstract

Particulate matter (PM) has been associated with a variety of adverse health effects primarily involving the cardiopulmonary system. However, the precise biological mechanisms to explain how exposure to PM exacerbates or directly causes adverse effects are unknown. Particles of varying composition may play a critical role in these effects. To study such a phenomenon, a simple, laminar diffusion flame was used to generate aerosols of soot and iron particles in the ultrafine size range. Exposures of healthy adult rats were for 6 h/day for 3 days. Conditions used included exposure to soot only, iron only, or a combination of soot and iron. We found animals exposed to soot particles at 250 $\mu g/m^3$ had no adverse respiratory effects. Exposure to iron alone at a concentration of 57 $\mu g/m^3$ also had no respiratory effects. However, the addition of 45 $\mu g/m^3$ of iron to soot with a combined total mass concentration of 250 $\mu g/m^3$ demonstrated significant pulmonary ferritin induction, oxidative stress, elevation of IL-1β, and cytochrome P450s, as well as activation of NFκB. These findings suggest that a synergistic interaction between soot and iron particles account for biological responses not found with exposure to iron alone or to soot alone.

Keywords: Particulate matter (PM); Iron; Soot; Interaction; Ferritin; Oxidative stress; NFκB

Introduction

Epidemiological studies strongly suggest statistically significant associations of adverse health effects in humans with exposure to particulate matter (PM) with a mass median aerodynamic diameter of 10 μm or less (PM_{10}). Inhalation of these particles into the respiratory tract at levels at or above the National Ambient Air Quality Standard of 150 $\mu g/m^3$ (averaged over a period of 24 h) has been associated with increased cardiopulmonary symptoms, as well as heightened morbidity and mortality in a wide range of subjects following short-term exposure to ambient particulate matter (Dockery and Pope, 1994; Pope et al., 1995). Effects have been noted in children, elderly individuals, and those with preexisting respiratory and cardiovascular disease. These individuals experience decrements in pulmonary function, exacerbation of breathing disorders including asthma and bronchitis, as well as cardiovascular problems, increased hospital admissions, and even a significant reduction in life expectancy. In addition, a recent study has shown antiviral responses of alveolar macrophages are adversely affected by exposure to PM_{10}, possibly leading to increased pulmonary infection in susceptible populations with suppressed or an immature immune response (Becker and Soukup, 1999).

Although there appears to be little doubt from the scientific literature that exposure to particulate matter poses a

* Corresponding author. Center for Health and the Environment, One Shields Avenue, University of California, Davis, CA 95616. Fax: +1-530-752-5300.

E-mail address: kepinkerton@ucdavis.edu (K.E. Pinkerton).

0041-008X/03/$ – see front matter © 2003 Elsevier Science (USA). All rights reserved.
doi:10.1016/S0041-008X(03)00157-1

potentially significant human health risk, there exists a number of major scientific uncertainties for PM health effects. Growing evidence supports the basic tenet that exposure to ambient PM exerts adverse consequences on public health, but the nature and severity of PM-associated human health effects have not yet been fully characterized. PM is a complex mixture containing organic compounds, soot, transition metals, sulfates, nitrates, as well as other trace elements (Hughes et al., 1998). Identification of toxic component(s) in PM responsible for particle-associated health effects has become an area of active investigation (Dreher et al., 1997; Saldiva et al., 2002). Specific particle compositions, such as transition metals, have been implicated in particle-induced pulmonary effects (Broeckaert et al., 1997, 1999; Pritchard et al., 1996; Rice et al., 2001). Interactions between various components may also account for PM-associated adverse effects. Hence, studies are needed to address the effects of particles of known composition and concentration. The elucidation of those potential mechanisms by which particles exert their effects requires studies using animal models exposed to particles under well-characterized and controlled conditions.

Iron is the predominant transition metal found in PM. Soot is also an important component of PM primarily composed of elemental carbon ranging from 3.5 to 17.5% of the total particle mass (Hughes et al., 1998; Cass et al., 2000). This study was designed to address three goals to study the health effects of inhaled particles in the lungs of young adult rats. (1) To determine the respiratory effects of short-term, repeated (3-day) exposure to airborne particles of soot or the transition metal iron in healthy adult rats. Measurements of lung injury, ferritin induction, oxidative stress, proinflammatory cytokines, NFκB activation, and histological features were used to define the acute respiratory toxicity and mechanisms following particle exposure to soot alone or to iron alone; (2) To identify the interaction between soot and iron particles by comparing the alterations of these biological responses in animals exposed to the combination of soot and iron particles with animals exposed to soot alone or iron alone; and (3) to determine the chemical and morphological characteristics of the iron/soot particle matrix formed during the process of fuel combustion. In this manner, we wished to elucidate and to better define potential mechanisms of putative interaction between mixed-particle compositions.

Materials and methods

Chemicals. Iron pentacarbonyl, ethylene, acetylene, reduced glutathione, glutathione disulfide (GSSG), glutathione reductase, 5,5′-dithio-bis(2-nitrobenzoic) acid (DTNB), 1-chloro-2,4-dinitrobenzene (CDNB), NADPH, 2-vinylpyridine, ferrous sulfate, ferric chloride, tripyridytriazine (TPTZ), and 5-bromo-2′deoxyuridine (BrdU) were purchased from Sigma-Aldrich Chemical Co. (St. Louis, MO).

Particle generation system. Most practical, high-temperature, industrial processes use hydrocarbon fuels that are not premixed with air. This form of combustion has been simulated with a laminar diffusion flame system that has been described in detail previously (Yang et al., 2001). Briefly, mixtures of acetylene and ethylene were used as fuels. Ethylene was the base fuel and acetylene was added as needed to compensate for the oxidation of soot by iron. In this manner, concentrations of soot and iron oxide particles in the postflame gases were controlled independently. Iron pentacarbonyl was introduced as a vapor by passing acetylene and ethylene over liquid iron pentacarbonyl. The particle emission from the flame was diluted by filtered air to bring the aerosol concentration to a level that could be maintained for the duration of short-term animal exposure studies. The system was operated to generate total constant concentrations of aerosol, while the iron loading could be varied from 40 to 100 $\mu g/m^3$ in the diluted postflame gases.

Samples of the flame-generated aerosols were collected on Teflon filters and 200-mesh holey carbon-coated copper grids. The morphology and phase of the particles collected from the exposure chambers were determined with a Philips EM-400 transmission electron microscope (TEM) operated at 100 kV. Morphology and chemical composition were determined with electron energy-loss spectroscopy (EELS) (Yang et al., 2001) using a JEOL JEM-200CX analytical electron microscope equipped with a Gatan 666 EELS spectrometer with 1.5 eV energy resolution. X-ray diffraction (XRD) results were obtained on a Scintag XDS 2000 X-ray diffractometer with copper tube. A differential mobility analyzer was used to measure the size distribution of the particles. X-ray fluorescence was used to measure the mass concentration of iron particles ($\mu g/m^3$).

Animals and inhalation system. Ten to 12-week-old male Sprague–Dawley rats weighing 260–310 g were purchased from Harlan Laboratories (Indianapolis, IN). All rats were housed in an animal facility with high-efficiency particulate air filters and were provided rat chow and water ad libitum. All animals were allowed to acclimate for 1 week prior to the onset of experimental exposures. Animals were handled in accordance with standards established by the U.S. Animal Welfare Acts as set forth in the National Institutes of Health Guidelines and by the University of California, Davis, Animal Care and Use Committee.

Animals were exposed by inhalation in sealed $20 \times 43 \times 18$ cm polycarbonate whole-body chambers to soot particles (total mass: 250 $\mu g/m^3$), iron particles (57 $\mu g/m^3$), or a combination of both soot and iron particles (iron: 45 $\mu g/m^3$, total mass: 250 $\mu g/m^3$) for 3 days, 6 h/day. Animals exposed to filtered air were used for each exposure. Three animals were housed in each chamber during exposure. Different sets of identical exposures were performed for bronchoalveolar lavage fluid (BALF) lung tissue, and histopathology and immunohistochemistry analyses.

BALF for cell viability and differentials. Preparation of BALF followed Harrod's protocol (Harrod et al., 1998). Briefly, within 2 hours following the end of particle exposure on the third day, rats were anesthetized with sodium pentobarbital (Nembutal; Cardinal Health, Sacramento, CA) and exsanguinated via the caudal aorta. The trachea was exposed, cannulated, and secured with a suture. The lungs were lavaged four times with a single volume of phosphate-buffered saline (Dulbecco's PBS, Mg^{2+} and Ca^{2+} free, pH 7.4; GibcoBRL, Grand Island, NY), 35 ml/kg body wt. Total cell count within BALF of each rat was determined using a hemocytometer. Cell viability was determined by trypan blue exclusion. Samples containing at least 5×10^4 cells each were spun down in duplicate onto glass slides using a Shandon Model 3 cytospin (Shandon Instruments, Pittsburgh, PA) and stained with Hema 3 (Fisher Scientific Company, Swedesboro, NJ) for determination of the proportion of macrophages, lymphocytes, and neutrophils. A minimum of 500 cells were counted from each cytospin slide.

Preparation of lung homogenates, microsomes, and nuclear extracts. Immediately following deep anesthesia and exsanguination via the caudal aorta, the lungs were removed from the thorax, frozen in liquid nitrogen, and subsequently homogenized in ice-cold Tris–HCl buffer (25 mM Tris, 1 mM EDTA, 10% glycerol, and 1 mM DTT, pH 7.4) with a glass homogenizer. The homogenate was centrifuged at 10,000*g* for 20 min at 4°C. The supernatant and sediment fractions were separated, and the supernatant was aliquoted and stored at −80°C. For microsomal fractions, the supernatant obtained as described above was further centrifuged at 105,000*g* for 75 min. The microsomal pellet was suspended in 0.05 M Tris–HCl buffer, pH 7.4, with 0.25 M sucrose. The crude nuclear fraction in the low-speed centrifugation was collected and washed with homogenate buffer containing Triton X-100 three times, followed by washing one time without Triton X-100. Nuclear protein was extracted with buffer C (20 mM Hepes, 25% glycerol, 0.42 M NaCl, and 1 mM EDTA) by centrifugation at 50,000*g* for 30 min.

Total protein, lactate dehydrogenase (LDH) activity in BALF. Measurement of total protein in the supernatant of BALF was performed by a modified Bradford assay according to the manufacturer's instructions (BioRad, Hercules, CA) with bovine serum albumin as a standard. The activity of LDH was measured using a colorimetric assay kit (Sigma-Aldrich) based on released LDH from the cytoplasm of damaged cells into BALF supernatant.

GSH assay. An aliquot of BALF was mixed with an equal volume of 6% metaphosphoric acid. After incubation on ice for 10 min, the mixture was centrifuged at 14,000*g* for 10 min and the supernatants were stored at −80°C prior to analysis. Lung tissues were homogenized with addition of 6% metaphosphoric acid, centrifuged, and stored at −80°C as described above. GSH was measured by an enzymatic method (Anderson, 1985; Tietz, 1969), using DTNB-oxidized glutathione reductase recycling assay. Reduced GSH was oxidized by DTNB to give GSSG with stoichiometric formation of 5-thio-2-nitrobenzoic acid (TNB). GSSG was reduced to GSH by the action of glutathione reductase and NADPH. The rate of TNB formation was measured at 412 nm and was proportional to the sum of GSH and GSSG present. GSSG was determined after treatment for derivatization with 2-vinylpyridine. The detection limit for GSH was 0.008 nmol/ml and 0.004 nmol/ml for GSSG in the final reaction medium.

Total antioxidant power. Total antioxidant power in BALF and lung homogenates was determined by ferric reducing/antioxidant power (FRAP) assay according to protocol (Benzie and Strain, 1999). Briefly, at low pH, ferric TPTZ (Fe^{3+}–TPTZ) complex is reduced to the ferrous form and monitored by measuring the change in absorption at 593 nm. The change in absorbance is directly related to the total reducing power of the electron-donating antioxidants present in the reaction mixture of biological samples.

Proinflammatory cytokines. The levels of proinflammatory cytokines IL-1β and TNF-α were assessed in lung homogenates by rat ELISA kits according to the manufacturer's instructions (R&D Systems, Minneapolis, MN). A 1:2 dilution of samples in calibrator diluent was used for cytokine determination. Quantitation of cytokines was normalized to total protein in the sample.

Western blot analysis for ferritin and CYP450s. Western blot analyses were used to measure levels of ferritin and cytochrome P450 (CYP) 1A1, 2B1, and 2E1 in the lungs. Lung homogenates (for ferritin) or microsomal proteins (for CYP450s) were loaded and separated on 10–12% SDS–PAGE, followed by transblotting to an ImmunBlot PVDF membrane (Bio-Rad, Hercules, CA). The membrane was subsequently probed with primary antibody against human ferritin (rabbit anti-human ferritin polyclonal antibody; Dako, Carpinteria, CA) or goat anti-rat CYP1A1, 2B1, and 2E1 (Daichi Pure Chemicals Co., Tokyo, Japan) at a dilution of 1:1000. Horseradish peroxidase-conjugated secondary antibody was added at 1:3000 dilution. The blots were subsequently developed using an enhanced chemiluminescence detection kit (AmerSham Pharmacia Biotech, Piscataway, NJ). Following exposure on autoradiography film, immunoreactive protein bands were quantified by densitometry.

NFκB–DNA binding activity. Electrophoretic mobility shift assay was performed to determine NFκB–DNA binding activity. The oligonucleotide used as a probe (Promega, Madison, WI) was double-stranded DNA containing the NFκB consensus sequence (5′-CCTGTGCTCCGGGAATTTCCCTGGCC-3′) labeled with [γ-^{32}P]dATP using T4 polynucleotide kinase. The binding reaction of nuclear proteins to the probe was assessed by incubation of mixtures

containing 5 μg nuclear protein, 0.5 μg poly (dl·dC) and 40,000 cpm ^{32}P-labeled probe in the binding buffer (7.5 mM HEPES, pH 7.6, 35 mM NaCl, 1.5 mM $MgCl_2$, 0.05 mM EDTA, 1 mM DTT, and 7.5% glycerol) for 30 min at 25°C. For the competitive assay, excessive unlabeled oligonucleotides were incubated with proteins prior to the addition of radiolabeled probe. Protein–DNA binding complex was separated by 5% polyacrylamide gel electrophoresis and autoradiographed overnight.

Lung fixation and histopathology. All lung tissues prepared for histological analysis were done under standard conditions. Animals were deeply anesthetized with an overdose of sodium pentobarbital. The trachea was exposed, cannulated, and secured with a suture. Prior to instillation of fixative, the diaphragm was ruptured to allow collapse of the lungs. The lungs were subsequently fixed with 1% paraformaldehyde/0.1% glutaraldehyde in situ at 30 cm of pressure for 1 h. The lungs and mediastinal contents were removed en bloc and stored in fixative. Lung tissue slices were prepared from both right and left lung lobes and embedded in glycomethacrylate. Sections 1.5-μm thick were prepared using a HM 355 rotary microtome (Carl Zeiss, Thornwood, NY). Airways, terminal bronchioles, and the lung parenchyma were examined microscopically for the presence of cellular changes and inflammation.

Immunohistochemistry for BrdU. Miniosmotic pumps containing BrdU were implanted subcutaneously 1 day prior to the onset of each experiment. Duodenum is used as a labeling control for each rat. As described above, following exposure, the lungs were inflation fixed via the trachea with 1% paraformaldehyde/0.1% glutaraldehyde for 1 h and sequentially transferred into 70, 95, and 100% ethanol. Tissues were embedded into paraffin and 5-μm-thick sections were prepared. Endogenous peroxidase activity was blocked with 3% hydrogen peroxide, followed by incubation with 0.1% protease for 30 min at 37°C. Following nonspecific blocking in 10% horse serum, sections were incubated with mouse monoclonal anti-BrdU primary antibody (Roche Diagnostic Corp., Indianapolis, IN) for 1 h at 37°C. Sections were subsequently incubated in biotinylated rabbit anti-mouse secondary antibody with Vectastain ABC kit (Vector, Burlingame, CA) for 30 min at room temperature. Diaminobenzidine (DAB) was used as chromogen substrate, while tissue counterstaining was done with nuclear fast red. Labeling indices were determined for the main axial airway path, airway bifurcations, terminal bronchioles, and the proximal alveolar regions (i.e., the alveoli within 400 μm distance of the terminal bronchiole). In each region, 500 to 1000 cells per lung were counted.

Statistics. Statistical analyses were performed using Staview computer software (SAS Institute, Cary, NC). The following statistical procedures were used: (1) Student's *t test* to compare the difference between each particle exposure group and the corresponding control group; (2) all parameters from each exposure were expressed as a percentage of the corresponding control group. ANOVA followed by Fisher's PLSD post hoc multiple comparisons were performed to evaluate differences among exposure to soot alone, iron alone, or the combination of soot and iron. All data were presented as the mean ± SE. Differences were considered significant at $p < 0.05$.

Results

Particle characterization

The average total mass concentration of iron generated in combination with soot was 45 μg/m^3. The overall total concentration of the combined iron and soot was 250 μg/m^3. For those experiments with exposure to only soot particles, the mass concentration was 250 μg/m^3. For the experiments in which animals were exposed only to iron particles, the total mass concentration of iron was 57 μg/m^3. The morphology of all samples as determined by the TEM consisted of crystalline iron oxide particles ranging in size from 10 to 50 nm in diameter, in aggregate with quasigraphitic carbon (Fig. 1A and B). Aggregate chains typical of combustion-generated soot were seen, with hexagonal- and rhomboidal-shaped iron oxide particles in some cases distinct from the carbon and in other cases dispersed throughout the soot. The iron/soot sample had a larger fraction of carbon, as well as larger sized iron oxide/carbon aggregates, compared to the iron only sample. Maximum aggregate size for the iron/soot sample was ~1 μm compared to 200 nm for the iron-only samples.

EELS demonstrated that the majority of particles containing iron were iron oxide in composition. Further analysis of the spectra for each of these particles demonstrated a ratio of iron to oxygen of approximately 0.5 to 0.7, suggesting that the actual composition of these particles was close to Fe_2O_3. Selected area diffraction patterns (Fig. 1C and D) confirmed the presence of γ-Fe_2O_3 (maghemite) for both the iron/soot and iron-only sample. The presence of d-spacing values in both the iron/soot and iron-only sample at 5.88, 4.82, 3.78, and 3.40 ÅA indicated γ-Fe_2O_3 (maghemite), since these values do not appear for Fe_3O_4 (magnetite). X-ray diffraction, which gave more precise values than electron diffraction, indicated maghemite as the only phase present in the iron-only sample. However, there was not enough signal to obtain XRD measurements on the iron/soot samples. Particle generation over the 3-day period of exposure, with daily exposures being 6 h each, yielded a highly consistent concentration of particulate material.

Measurement of lung injury in BALF

Inhalation of soot particles alone (250 μg/m^3), iron particles alone (57 μg/m^3), or the combination of soot plus iron

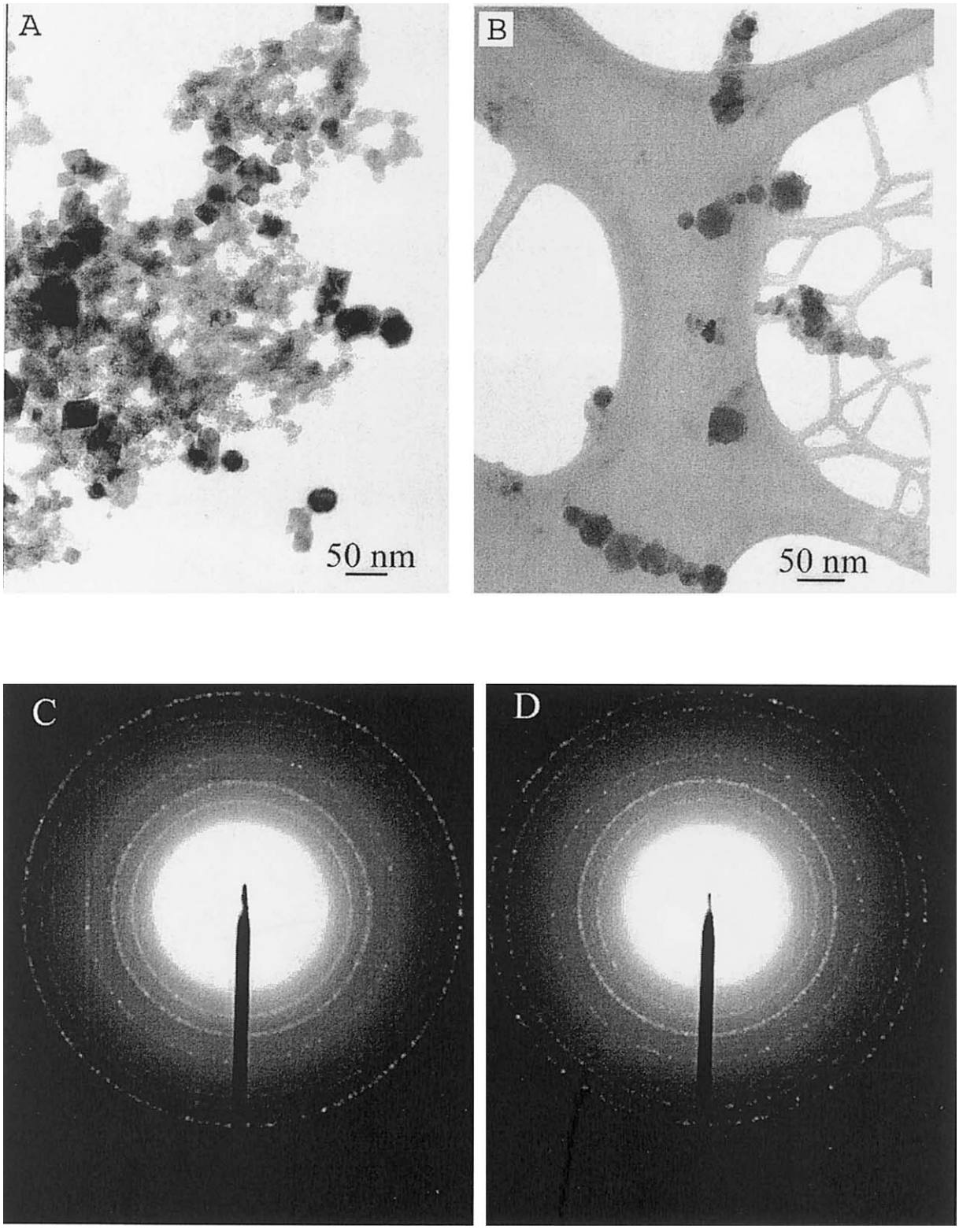

Fig. 1. Bright-field transmission electron micrographs of (A) soot + iron and (B) iron only samples. Iron oxide crystals are 10–50 nm in diameter. Note the presence of more soot and larger iron oxide/soot agglomerates in the iron/soot sample. Selected area diffraction patterns for the iron/soot sample (C) and iron only sample (D) are also shown and in both cases match the γ-Fe_2O_3 (maghemite) phase.

particles (45 $\mu g/m^3$ of iron, 250 $\mu g/m^3$ total particulate mass) demonstrated no significant changes from control in the level of protein and in the activity of LDH within BALF (Fig. 2). No significant changes were found in the number of total cells, percentage of viable cells (i.e., viability), or the percentages of macrophages, neutrophils, and lymphocytes

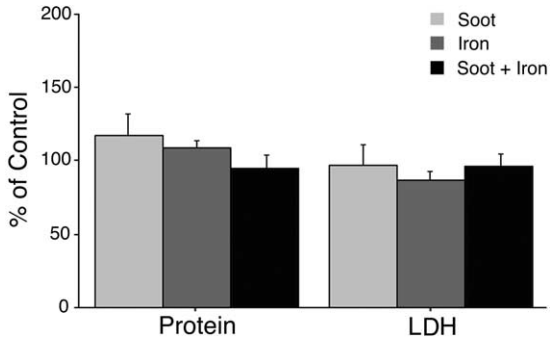

Fig. 2. Total protein levels and LDH activity in BALF following exposure to soot alone, iron alone, or soot + iron. The controls are taken as 100%. Control values for protein (μg/ml) were 101 ± 15, 114 ± 3, and 78 ± 4 corresponding to soot alone, iron alone, or soot + iron. Control values for LDH (U/L) were 1.24 ± 0.17, 1.45 ± 0.17, and 2.61 ± 0.54 corresponding to soot alone, iron alone, or soot + iron.

recovered from BALF following exposure to each of the different particle compositions (data not shown).

Ferritin

The level of ferritin in lung homogenates was measured as an indicator of iron bioavailability following exposure. Significant elevation of ferritin levels was noted only in animals exposed to soot plus iron particles (2.6-fold) compared with filtered air controls. The induction of ferritin in animals exposed to soot plus iron was significantly different from animals exposed to soot alone or iron alone (Fig. 3).

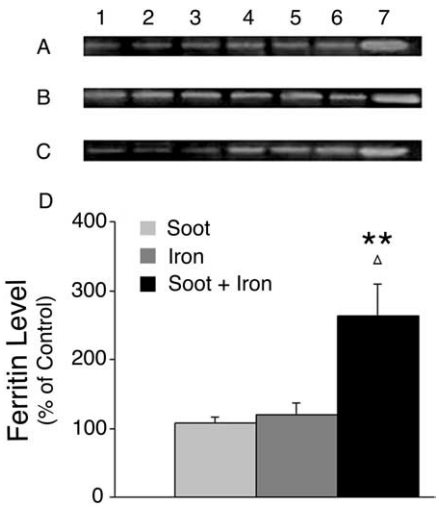

Fig. 3. Western blot of ferritin expression in lung homogenages following exposure to soot (A), iron (B), or soot + iron (C). Lanes 1–3, control animals; lanes 4–6, particle-exposed animals, and lane 7, positive control with purified human liver ferritin. Relative band intensity of ferritin expression by imaging densitometry (D). The corresponding controls run simultaneously with each different particle exposure group are taken as 100%. **Significant difference from soot alone ($p < 0.01$). $^{\Delta}$ Significant difference from iron alone ($p < 0.05$).

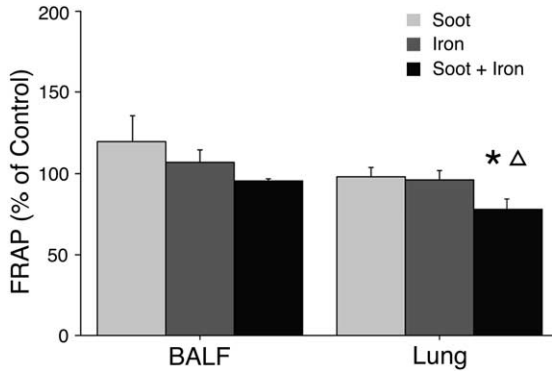

Fig. 4. Ferric-reducing antioxidant power in BALF and lung tissue following exposure of rats to different particle compositions. The controls are taken as 100%. Control values were 5.0 ± 0.4, 4.4 ± 0.5, and 9.1 ± 0.1 in BALF (nmol/ml) and 578 ± 34, 286 ± 14, and 540 ± 22 in lung tissue (nmol/mg protein), corresponding to soot alone, iron alone, or soot + iron. *Significant difference from soot alone ($p < 0.05$). $^{\Delta}$Significant difference from iron alone ($p < 0.05$).

Oxidative stress

Total antioxidant power measured by FRAP assay and glutathione redox status were used as indicators of oxidative stress. Exposure to the combination of soot plus iron particles demonstrated a significant reduction in FRAP levels in both BALF (control: 9.09 ± 0.12 nmol/ml, soot+iron: 8.64 ± 0.11 nmol/ml) and lung tissues (control: 540 ± 22 nmol/mg protein, soot+iron: 422 ± 32 nmol/mg protein). In contrast, animals exposed to soot alone or iron alone showed no differences in FRAP levels compared to their control animals. When these same values were expressed as a percentage of control, it was found that the FRAP value within the lung tissues of animals exposed to soot plus iron was significantly reduced from the animals exposed to soot alone or to iron alone (Fig. 4). Glutathione levels, both the reduced form as well as the oxidized form, were measured in BALF and lung tissue. No significant changes were noted in GSH levels following exposure to any combination of airborne particles. In contrast, the level of GSSG demonstrated a statistically significant increase for animals exposed to the mixture of soot and iron in BALF (control: 0.029 ± 0.005 nmol/ml, soot+iron: 0.086 ± 0.016 nmol/ml). No differences were noted for animals exposed to iron alone or soot alone. The ratio of GSSG to GSH (glutathione redox ratio, GRR) also demonstrated a significant increase only in animals exposed to the combination of soot plus iron particles both in BALF (control: 0.105 ± 0.016, soot+iron: 0.177 ± 0.029) and in lung tissues (control: 0.051 ± 0.01, soot+iron: 0.096 ± 0.017). When these values were expressed as a percentage of control within BALF, it was observed that the level of GSSG in animals exposed to soot plus iron was significantly elevated from the animals exposed to soot alone or iron alone (Fig. 5A). In addition, the elevation of GSSG and GRR within lung tissues was also

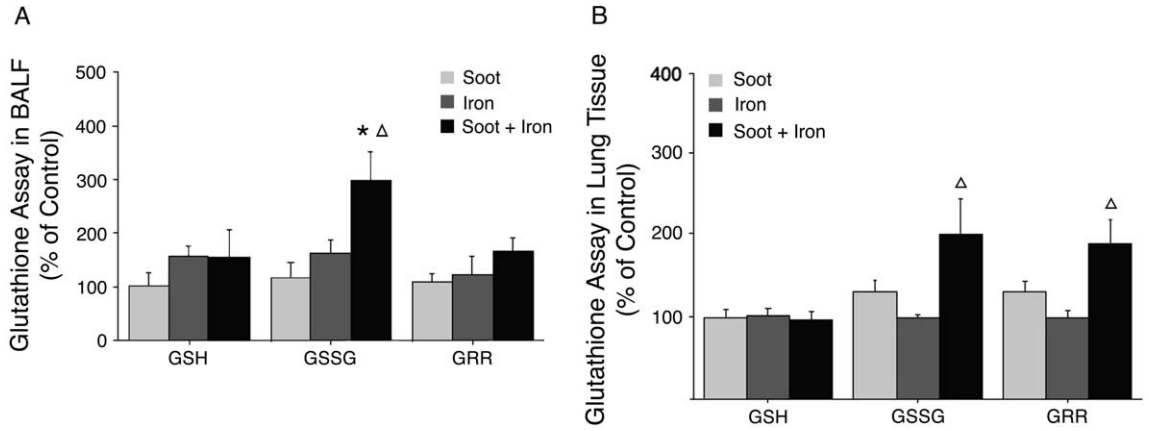

Fig. 5. Changes in GSH, GSSG, and GSSG/GSH (GRR) following exposure of rats to different particle compositions in BALF (A) and lung tissue (B). The controls are taken as 100%. Control values for GSH were 0.429 ± 0.076, 0.553 ± 0.118, and 0.344 ± 0.118 in BALF (nmol/ml) and 93.9 ± 5.1, 112.4 ± 7.7, and 118.2 ± 17.9 in lung tissue (nmol/mg protein), corresponding to soot alone, iron alone, or soot + iron. Control values for GSSG were 0.082 ± 0.014, 0.035 ± 0.008, and 0.029 ± 0.005 in BALF (nmol/ml) and 16.2 ± 0.9, 13.7 ± 0.6, and 5.7 ± 1.4 in lung tissue (nmol/mg protein), corresponding to soot alone, iron alone, or soot + iron. Control values for GRR were 0.166 ± 0.022, 0.071 ± 0.018, and 0.105 ± 0.016 in BALF and 0.149 ± 0.012, 0.112 ± 0.008, and 0.051 ± 0.010 in lung tissue, corresponding to soot alone, iron alone, or soot + iron. *Significant difference from soot alone ($p < 0.01$). $^{\Delta}$Significant difference from iron alone ($p < 0.05$).

observed in animals exposed to soot plus iron particles compared with iron-only exposure (Fig. 5B).

Proinflammatory cytokines

Proinflammatory cytokines for IL-1β and TNF-α within lung tissue were measured following particle exposure. IL-1β was significantly increased following exposure to the combination of soot plus iron (controls: 34.9 ± 0.2 pg/mg protein, soot+iron: 43.9 ± 2.5 pg/mg protein) but was not changed to a significant degree from control values following exposure to soot alone or iron particles alone. The change of IL-1β in animals exposed to soot plus iron was significantly increased from that of animals exposed to soot alone or iron alone (Fig. 6A). No statistically significant differences were noted in values of TNF-α within any of the exposure groups (Fig. 6B).

NFκB–DNA binding activity

To examine the effects of particle exposure on NFκB activation, NFκB–DNA binding activity was measured in lung tissue nuclear extract. Exposure to soot particles alone or exposure to iron particles alone did not significantly change NFκB–DNA binding activity within the lung tissues of these animals (Fig. 7A and B). In contrast, exposure of animals to soot plus iron resulted in a significant increase of NFκB–DNA binding activity (Fig. 7C), and the activation was significantly increased from the animals exposed to soot alone or iron alone (Fig. 7D).

Cytochrome P450 monooxygenase isoforms

Microsomal fractions of lung tissues were used to measure the levels of three major isoforms of cytochrome P450,

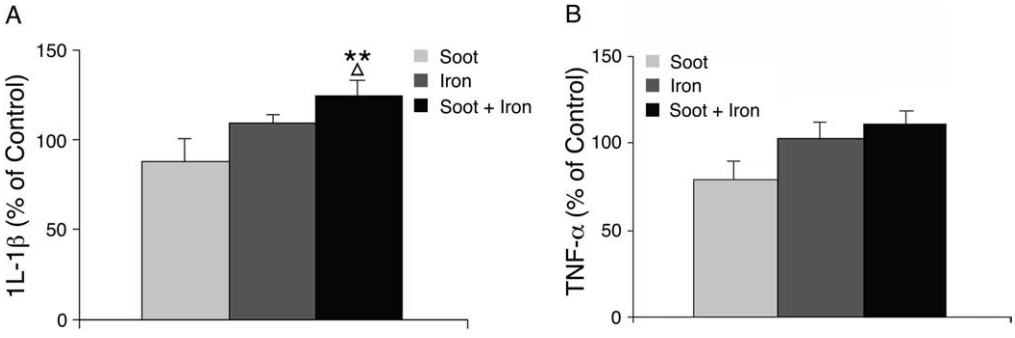

Fig. 6. Protein levels of IL-1β (A) and TNF-α (B) in lung homogenates of rats following exposure to different particle compositions were measured by ELISA. The controls are taken as 100%. Control values for IL-1β (pg/mg protein) were 43.3 ± 8.5, 30.1 ± 2.8, and 34.9 ± 0.5, corresponding to soot alone, iron alone, or soot + iron. Control values for TNF-α (pg/mg protein) were 18.3 ± 4.2, 19.3 ± 2.3, and 24.0 ± 2.9, corresponding to soot alone, iron alone, or soot + iron. **Significant difference from soot alone ($p < 0.01$). $^{\Delta}$Significant difference from iron alone ($p < 0.05$).

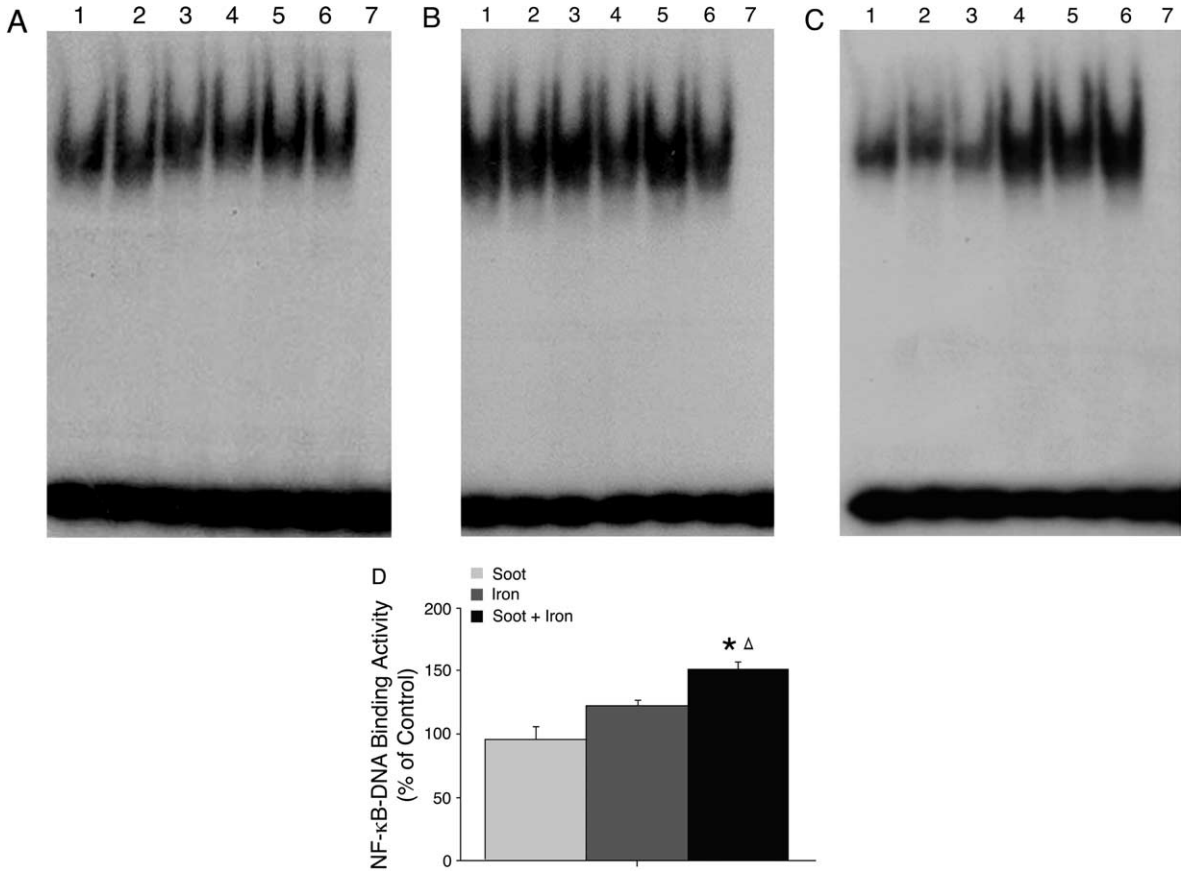

Fig. 7. Electrophoretic mobility shift assay to show effects of exposure to soot (A), iron (B), or soot and iron (C) on NFκB-DNA binding activity. Lanes 1–3, control animals; lanes 4–6, exposure animals; lane 7, competition assay. Relative band intensity of NF-κB–DNA binding activity by imaging densitometry (D). The corresponding controls from each individual particle exposure are taken as 100 %. *Significant difference from soot alone ($p < 0.01$). $^{\Delta}$Significant difference from iron alone ($p < 0.05$).

1A1, 2B1, and 2E1. Exposure to soot particles (Fig. 8A) or iron particles (Fig. 8B) demonstrated no significant alterations in any of these isoforms following exposure. In contrast, exposure to the combination of soot plus iron demonstrated significant increases in the levels of cytochrome P450 1A1(3.2-fold), as well as 2E1 (1.5-fold) within lung microsomes (Fig. 8C). Although the level of the isoform 2B1 was also elevated, it failed to attain a level of statistical

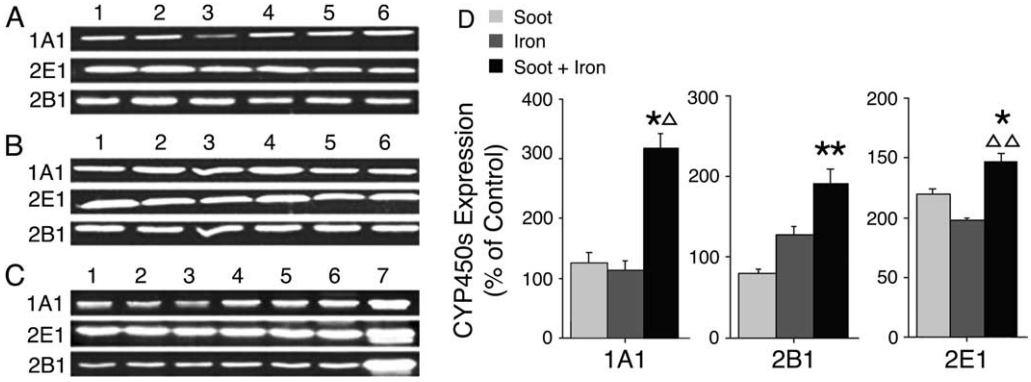

Fig. 8. Effects of exposure to soot alone (A), iron alone (B), or soot and iron (C) on pulmonary cytochrome CYP450 1A1, 2B1, and 2E1 were detected by Western blot analysis. Lanes 1–3, control animals; lanes 4–6, exposure animals; lane 7, positive controls of 1A1, 2B1, and 2E1. Relative band intensity of CYP 450s by imaging densitometry (D). The corresponding controls from each individual particle exposure are taken as 100%. *Significant difference from soot alone ($p < 0.05$). **Significant difference from soot alone ($p < 0.01$). $^{\Delta}$ Significant difference from iron alone ($p < 0.05$). $^{\Delta\Delta}$Significant difference from iron alone ($p < 0.01$).

significance. When these alterations were compared among different particle exposures, as the values expressed as a percentage of control, it was found that the induction of 1A1 and 2E1 in animals exposed to the soot plus iron was significantly different from the animals exposed to soot alone or iron alone (Fig. 8D). The level of 2B1 in the soot plus iron group was also significantly different from soot alone (Fig. 8D).

Lung histopathology and BrdU immunolabeling

Extensive analyses of specific anatomical sites within the respiratory tract of animals were examined for the pulmonary bronchial tree and parenchyma. The anatomical appearance of terminal bronchioles as well as the lung parenchyma immediately beyond these terminal bronchioles in the lungs of animals exposed to filtered air, soot, or soot plus iron is illustrated in Fig. 9. We were unable to observe any significant changes within the anatomical structure of the terminal bronchioles within any of these animals (Fig. 9A, C, and E). Within the parenchyma we also failed to detect obvious differences in septal wall structure (Fig. 9B and D); however, it was noted that there was a subtle increase in septal wall thickness within patchy areas of those animals exposed to iron plus soot particles (Fig. 9F).

Immunohistochemical staining to examine the uptake of BrdU within specific anatomical sites was done for two groups of animals, those exposed to filtered air (control) and those exposed to the combined soot and iron particles. Anatomical analysis included examination of epithelium of the conducting airways as well as the epithelial lining over airway bifurcations and underlying interstitial cells, terminal bronchioles, and proximal alveolar regions. These studies failed to demonstrate significant differences in the incorporation of BrdU into epithelial and/or interstitial cells of the conducting airways or the cells of the proximal alveolar region following particle exposure compared with control animals (data not shown).

Discussion

Transition metal-mediated generation of ROS and oxidative stress have been proposed as one of the main mechanisms for PM toxicity (Dye et al., 1997, 1999; Jimenez et al., 2000; Kennedy et al., 1998; Kodavanti et al., 1998; Li et al., 1996). Due to the complexity of PM, it is critical to characterize and to identify the biological activities of individual components of PM to elucidate PM-associated effects. Biological responses to inhaled PM not only depend upon individual constituents, but also upon the interplay between individual components. Following 3 days exposure to soot particles alone at a concentration of 250 $\mu g/m^3$ or to iron particles alone at 57 $\mu g/m^3$, our studies have shown that there were no significant changes in lung injury, ferritin induction, oxidative stress, NFκB activation, proinflammatory cytokines, or cytochrome P450s in the lungs of these exposed healthy adult rats. However, when animals were exposed to combined soot and iron particles at an identical total mass concentration of 250 $\mu g/m^3$ with a slightly lower concentration of iron (45 $\mu g/m^3$), significant alterations were observed in these animals. These results demonstrated that a synergistic interaction exists between soot and iron particles, i.e., none of the individual constituents have an effect when given alone but, when combined, produce a significant response (Schlesinger, 1995).

We postulate that the mechanisms underlying the synergistic interaction between these two components are both chemical and physical. The iron generated under our experimental conditions was iron oxide (Fe_2O_3). Iron oxide is considered to be nontoxic and of low bioavailability (Stokinger, 1984). In a study with hamsters, intratracheal instillation of 50 mg Fe_2O_3 failed to produce any long-term adverse health effects (Saffiotti et al., 1972). A recent study reported that Fe_2O_3 particles purchased commercially were not capable of oxidant generation and did not induce an inflammatory response (Lay et al., 1999). Our study showed exposure to iron particles alone (57 $\mu g/m^3$) did not induce increased expression of intracellular ferritin, an indicator of bioavailable iron following exposure (Fang and Aust, 1997; Smith and Aust, 1997). Hence, no catalytic active iron was available for electron transfer and therefore capable of participation in the Fenton reaction leading to the production of ROS (Imlay et al., 1998; Lucesoli et al., 1999; Halliwell, 1991). This was confirmed by the absence of oxidative stress, lung injury, proinflammatory cytokine elevation, or NFκB activation.

Exposure to soot alone at a concentration of 250 $\mu g/m^3$ also failed to demonstrate any adverse respiratory effects. Soot is considered to be an inert particle that has little effect when inhaled alone (Schlesinger, 1995). In a number of animal inhalation studies, no changes were noted in the respiratory system of animals when exposed to carbon black at 10 mg/m^3 (Jakab, 1992, 1993; Jakab and Hemenway, 1994). However, in the present study, exposure to a mixture of soot and iron particles resulted in significant responses that were not found with exposure to iron alone or soot alone. This synergism could be due to the fact that soot may serve as a reductant and could lead to the reduction of iron oxide (Boncyzk, 1991; Ritrievi et al., 1987; Zhang and Megaridis, 1996). Alternatively, soot could act as a carrier for iron particles. Fig. 1 illustrates that aggregates were formed in the mixture of soot and iron particles. Studies with aggregated ultrafine particles have shown significantly greater biological potency (Lee et al., 1985; Heinrich et al., 1995). In our study, these soot/iron aggregates may influence both soot and iron particles to deposit at similar sites in the lungs, where the chemical interaction between both particles could persist. It is also possible that soot particles could impede clearance of iron particles from the lungs, thus allowing for particle solubilization and/or conversion of the iron to a more biologically active form.

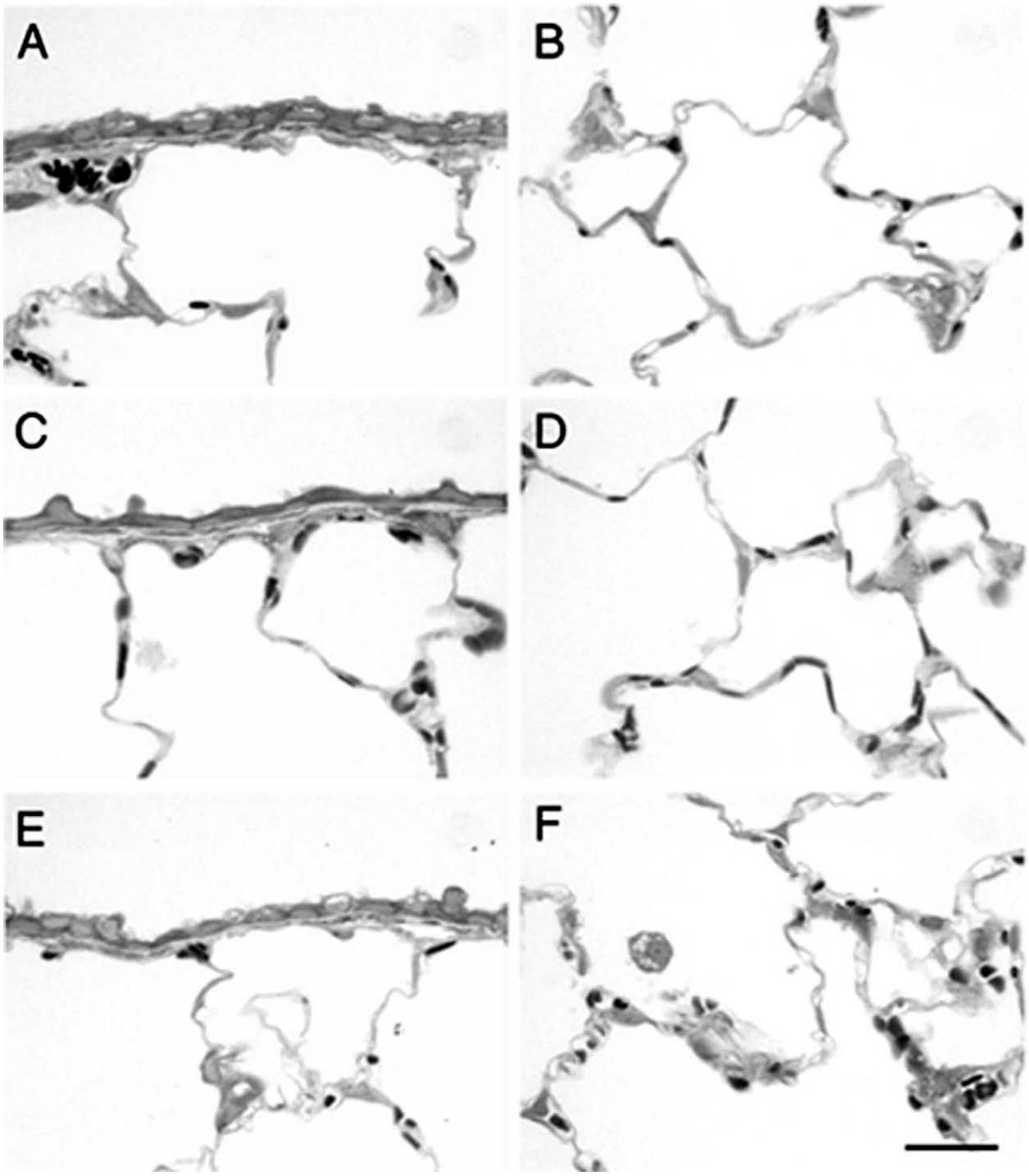

Fig. 9. Light micrographs of terminal bronchioles (A, C, and E) and alveolar parenchyma (B, D, and F) from rat lungs following exposure to filtered air (A and B), soot (C and D), or iron and soot (E and F). Bar represents 20 μm.

The interaction between soot and iron particles allows iron to become bioavailable, as indicated by the induction of intracellular ferritin. Catalytic iron is capable of redox cycling, resulting in the generation of ROS and oxidative stress in the lungs of rats, demonstrated by a significant decrease in total antioxidant power (FRAP) and changes in glutathione redox status following exposure to soot plus iron particles. Glutathione is a critical antioxidant in the lungs that accounts for 90% of intracellular nonprotein thiols and protects cells from oxidative damage (Kelly, 1999; Rahman and MacNee, 1999). Changes in glutathione redox status, include reduced GSH, oxidized GSH (GSSG), and the ratio of GSSG/GSH, can be used as markers of oxidative stress. Nuclear factor κB, a pivotal transcription

factor involved in the regulation of oxidative stress, inflammatory, and immune responses, is a sensor when oxidative stress occurs. Excessive release of ROS and alteration of glutathione redox status could trigger the signal transduction pathway leading to activation of NFκB (Li and Karin, 1999; Rahman, 2000; Rahman and MacNee, 2000).

Expression of many proinflammatory mediators such as cytokines (IL-1β, TNF-α, and IL-6), chemokines (IL-8 and MIP-2), adhesion molecules (VCAM-1, ICAM-1, and E-selectin), and enzymes (iNOS) are regulated by NFκB (Barnes and Karin, 1997; Christman et al., 1998). Our data show NFκB–DNA binding activity is significantly increased, accompanied by an elevation of IL-1β, indicating the activation of NFκB signaling in the lungs of rats following exposure to combined soot and iron particles. Studies have demonstrated that in vitro and in vivo PM exposure, including residual oil fly ash (ROFA) and PM_{10}, resulted in activation of NFκB (Jimenez et al., 2000; Kang et al., 2000; Kennedy et al., 1998; Quay et al., 1998; Samet et al., 2002). Carter et al. (1997) and Quay et al. (1998) observed gene expression of NFκB-dependent proinflammatory cytokines was induced following ROFA exposure. Kodavanti and colleagues (1997) found the mRNA levels of IL-1, IL-6, and MIP-2, but not TNF-α, were induced by ROFA. In the present study we also found the significant induction of IL-1β, but not TNF-α. Differential expression and synthesis of proinflammatroy cytokines could imply a multi-factorial regulation of gene expression. Aside from NFκB, other transcription factors such as activator protein -1, interferon regulatory factors, and signal transducers and activators of transcription are also involved in the induction of proinflammatory cytokines (Julkunen et al., 2001). The concentration of PM exposure may also affect the expression of proinflammatory mediators. Dye et al. (1999) found that rat tracheal epithelial (RTE) cells exposed to ROFA at 5 or 10 $\mu g/cm^2$ were associated with an increase in mRNA levels for limited number of mediators; however, when RTE cells were exposed to ROFA at 20 $\mu g/cm^2$, a significant increase in mRNA levels for all mediators (IL-6, MIP-2, and iNOS) was observed. In our study, we measured protein levels of IL-1β and TNF-α following particle exposure, but only IL-1β was found to be significantly increased. Although we would have expected a similar increase in TNF-α, it is likely that the complexity of cytokine gene expression or different levels of activation by NFκB for different cytokines may account for this disparity in cytokine induction observed following exposure to the combination of soot and iron particles.

It has been found that PM exposure is not only associated with pulmonary effects, but also cardiovascular events such as increased fibrinogen levels, increased plasma viscosity, systemic oxidative stress, and decreased heart-rate variability in healthy and cardiovascular compromised humans and rats (Kodavanti et al., 2000, 2002; Peters et al., 1997; Pope et al., 1999; Ulrich et al., 2002). The release of NFκB-dependent proinflammatory cytokines from the pulmonary system into the circulation is thought to play an important role in the progression of cardiovascular diseases. These cytokines stimulate the synthesis of fibrinogen, tissue factor, regulate the expression of thrombomodulin, and stimulate the bone marrow response, which in turn causes cardiac effects (van Eden and Hogg, 2002; Sharma et al., 2000; Cicala and Cirino, 1998). NFκB-dependent adhesion molecules may also concomitantly alter fibrin degradation and/or stimulate synthesis of fibrinogen. Further, the induction of NFκB-regulated iNOS could increase the synthesis of NO, a potent vasodilating compound, and impair the normal function of the blood pressure regulating system. Therefore, it is possible, through the activation of NFκB in the lungs of rats exposed to iron and soot particles, gene expression could be altered, which may affect the cardiopulmonary systems. Using a rat cardiopulmonary cDNA array, Nadadur and Kodavanti (2002) examined gene expression profiles in rat lungs exposed to ROFA and demonstrated ROFA- and metal-specific increased expression of lung injury/inflammation, stress response, and repair-related genes. They also found genes involved in vascular contractility, thromogenic activity, cytokines, and adhesion molecules were also induced following exposure.

Significant increases in the levels of two major isoforms of the cytochrome P450 (1A1 and 2E1) within the lungs were also found following exposure to combined soot and iron particles. Exposure to soot at an identical mass concentration (250 $\mu g/m^3$) in the absence of iron failed to elicit changes in CYP 450 1A1, 2E1, or 2B1. Exposure to iron alone also failed to induce changes in these cytochrome P450 isoforms. Tests were done to determine whether the soot fraction generated under our combustion conditions produced polyaromatic hydrocarbons (PAHs). Such compounds possess the ability to induce cytochrome P450, especially the isoform of 1A1. Analysis of soot extracts for 16 polyaromatic hydrocarbons arising from a hydrocarbon combustion process (benzo[*a*]pyrene, benzo[*a*]anthracene, benzo[*b*]fluoranthene, benzo[*g,h,l*]perylene, benzo[*k*]fluoranthene, acenaphthene, anthracene, acenaphthylene, naphthalene, chrysene, dibenz[*a,h*]anthracene, fluoranthene, fluorene, indeno[*1,2,3-cd*]pyrene, phenanthrene, and pyrene) failed to detect any levels of these PAHs. In light of the catalytic oxidation expected with iron present in the fuel, it is not surprising that PAHs were not detectable. It is therefore unlikely that PAHs or soot are the cause of the P450 response. Induction of CYP 1A1 and 2E1 by combined soot and iron exposure, but not by soot alone or iron alone, suggests that bioavailable iron is responsible for this heme-thiolate protein response. A study done by Shaw and colleagues (1997) also found that iron induced expression of cytochrome P450s in a dose-dependent manner.

In conclusion, to the best of our knowledge, this is the first report using laboratory-generated particles to investigate iron particles and their interaction with soot in the respiratory system of rats. We have demonstrated that, through synergistic interaction with soot, bioavailable iron

is responsible for induction of ferritin, oxidative stress, elevation of IL-1β, and NFκB activation in the lungs of healthy adult rats. These findings provide further evidence to support the hypothesis that transition metals interacting with other components may underlie PM-associated respiratory effects.

Acknowledgments

The authors thank Chuck Echer and the National Center for Electron Microscopy at the Lawrence Berkeley National Laboratory under U.S. Department of Energy Contract DE-AC-03-76SF00098. The authors also thank Stephen V. Teague for the design and construction of the animal exposure units used in this study, Dale Uyeminami for the operation of the diffusion flame system, and Janice L. Peake for expert technical assistance in photomicrography. This research was supported in part by Health Effects Institute Contract 97-8 and U.S. Environmental Protection Agency STAR Grants 827995 and 829215. Although the research described in this article has been funded in part by the U.S. Environmental Protection Agency, it has not been subjected to the Agency's required peer and policy review and therefore does not necessarily reflect the views of the Agency and no official endorsement should be inferred.

References

Anderson, M.E., 1985. Determination of glutathione and glutathione disulfide in biological samples. Methods Enzymol. 113, 548–555.

Barnes, P.J., Karin, M., 1997. Nuclear factor-kappaB: a pivotal transcription factor in chronic inflammatory diseases. N. Engl. J. Med. 336, 1066–1071.

Becker, S., Soukup, J.M., 1999. Exposure to urban air particulates alters the macrophage-mediated inflammatory response to respiratory viral infection. J. Toxicol. Environ. Health A 57, 445–457.

Benzie, I.F.F., Strain, J.J., 1999. Ferric reducing/antioxidant power assay: direct measure of total antioxidant activity of biological fluids and modified version for simultaneous measurement of total antioxidant power and ascorbic acid concentration. Methods Enzymol. 299, 15–27.

Bonczyk, P.A., 1991. Effect of ferrocene on soot in a prevaporized isooctane/air diffusion flame. Combust. Flame 87, 233–244.

Broeckaert, F., Buchet, J.P., Delos, M., Yager, J.W., Lison, D., 1999. Coal fly ash- and copper smelter dust-induced modulation of ex vivo production of tumor necrosis factor-alpha by murine macrophages: effects of metals and overload. J. Toxicol. Environ. Health A 56, 343–360.

Broeckaert, F., Buchet, J.P., Huaux, F., Lardot, C., Lison, D., Yager, J.W., 1997. Reduction of the ex vivo production of tumor necrosis factor alpha by alveolar phagocytes after administration of coal fly ash and copper smelter dust. J. Toxicol. Environ. Health 51, 189–202.

Carter, J.D., Ghio, A.J., Samet, J.M., Devlin, R.B., 1997. Cytokine production by human airway epithelial cells after exposure to an air pollution particle is metal-dependent. Toxicol. Appl. Pharmacol. 146, 180–188.

Cass, G.R., Hughes, L.A., Bhave, P., Kleeman, M.J., Allen, J.O., Salmon, L.G., 2000. The chemical composition of atmospheric ultrafine particles. Philos. Trans. R. Soc. Lond. A 358, 2582–2592.

Christman, J.W., Lancaster, L.H., Blackwell, T.S., 1998. Nuclear factor κB: a pivotal role in the systemic inflammatory response syndrome and new target for therapy. Intensive Care Med. 24, 1131–1138.

Cicala, C., Cirino, G., 1998. Linkage between inflammation and coagulation: an update on the molecular basis of the crosstalk. Life Sci. 62, 1817–1824.

Dockery, D.W., Pope III, C.A., 1994. Acute respiratory effects of particulate air pollution. Annu. Rev. Public Health 15, 107–132.

Dreher, K.L., Jaskot, R.H., Lehmann, J.R., Richards, J.H., McGee, J.K., Ghio, A.J., Costa, D.L., 1997. Soluble transition metals mediate residual oil fly ash induced acute lung injury. J. Toxicol. Environ. Health 50, 285–305.

Dye, J.A., Adler, K.B., Richards, J.H., Dreher, K.L., 1997. Epithelial injury induced by exposure to residual oil fly-ash particles: role of reactive oxygen species. Am. J. Respir. Cell Mol. Biol. 17, 625–633.

Dye, J.A., Adler, K.B., Richards, J.H., Dreher, K.L., 1999. Role of soluble metals in oil fly ash-induced airway epithelial injury and cytokine gene expression. Am. J. Physiol. Lung Cell Mol. Physiol. 277, L498–L510.

Fang, R., Aust, A.E., 1997. Induction of ferritin synthesis in human lung epithelial cells treated with crocidolite asbestos. Arch. Biochem. Biophys. 340, 369–375.

Halliwell, B., 1991. Reactive oxygen species in living system: source, biochemistry, and role in human disease. Am. J. Med. 91 (Suppl. 3c), 145–225.

Harrod, K.S., Mounday, A.D., Stripp, B.R., Whitsett, J.A., 1998. Clara cell secretory protein decreases lung inflammation after acute virus infection. Am. J. Physiol. Lung Cell Mol. Physiol. 275, L924–L930.

Heinrich, U., Fuhst, R., Rittinghausen, S., Cruetzenberg, O., Bellmann, B., Koch, W., Levsen, K., 1995. Chronic inhalation exposure of Wistar rats and two different strains of mice to diesel engine exhaust, carbon black, and titanium dioxide. Inhal. Toxicol. 7, 533–556.

Hughes, L.S., Cass, G.R., Jones, J., Ames, M., Olmez, L., 1998. Physical and chemical characterization of atmospheric ultrafine particles in the Los Angeles area. Environ. Sci. Technol. 32, 1153–1161.

Imlay, J.A., Chin, S.M., Linn, S., 1998. Toxic DNA damage by hydrogen peroxide through the Fenton reaction in vivo and in vitro. Science 240, 640–642.

Jakab, G.J., 1992. Relationship between carbon black particulate-bound formaldehyde, pulmonary antibacterial defenses and alveolar macrophage phagocytosis. Inhal. Toxicol. 4, 325–342.

Jakab, G.J., 1993. The toxicological interactions resulting from inhalation of carbon black and acrolein on pulmonary antibacterial and antiviral defenses. Toxicol. Appl. Pharmacol. 121, 167–175.

Jakab, G.J., Hemenway, D.R., 1994. Concomitant exposure to carbon black particulates enhances ozone-induced lung inflammation and suppression of alveolar macrophage phagocytosis. J. Toxicol. Environ. Health 41, 221–231.

Jimenez, L.A., Thompson, J., Brown, D.A., Rahman, I., Antonicelli, F., Duffin, R., Drost, E.M., Hay, R.T., Donaldson, K., MacNee, W., 2000. Activation of NF-κB by PM_{10} occurs via an iron-mediated mechanism in the absence of IκB degradation. Toxicol. Appl. Pharmacol. 166, 101–110.

Julkunen, I., Sareneva, T., Pirhonen, J., Ronni, T., Melen, K., Matikainen, S., 2001. Molecular pathogenesis of influenza A virus infection and virus-induced regulation of cytokine gene expression. Cytokine Growth Factor Rev. 12, 171–180.

Kang, J.L., Go, Y.H., Hur, K.C., Castranova, V., 2000. Silica-induced nuclear factor-kB activation: involvement of reactive oxygen species and protein tyrosine kinase activation. J. Toxicol. Environ. Health A 60, 27–46.

Kelly, F.J., 1999. Glutathione: in defense of the lung. Food Chem. Toxicol. 37, 963–966.

Kennedy, T., Ghio, A.J., Reed, W., Samet, J., Zagorski, J., Quay, J., Carter, J., Dailey, L., Hoidal, J.R., Devlin, R.B., 1998. Copper-dependant inflammation and nuclear factor-κB activation by particulate air pollution. Am. J. Respir. Cell Mol. Biol. 19, 366–378.

Kodavanti, U.P., Hauser, R., Christiani, D.C., Meng, Z.H., McGee, J., Ledbetter, A., Richards, J., Costa, D.L., 1998. Pulmonary responses to oil fly ash particles in the rat differ by virtue of their specific soluble metals. Toxicol. Sci. 43, 204–212.

Kodavanti, U.P., Jaskot, R.H., Costa, D.L., Dreher, K.L., 1997. Pulmonary proinflammatory gene induction following acute exposure to residual oil fly ash: roles of particle-associated metals. Inhal. Toxicol. 9, 679–701.

Kodavanti, U.P., Schladweiler, M.C., Ledbetter, A.D., Hauser, R., Christiani, D.C., McGee, J., Richards, J.R., Costa, D.L., 2002. Temporal association between pulmonary and systemic effects of particulate matter in healthy and cardiovascular compromised rats. J. Toxicol. Environ. Health A 65, 1545–1569.

Kodavanti, U.P., Schladweiler, M.C., Ledbetter, A.D., Watkinson, W.P., Campen, M.J., Winsett, D.W., Richards, J.R., Crissman, K.M., Hatch, G.E., Costa, D.L., 2000. The spontaneously hypertensive rat as a model of human cardiovascular disease: evidence of exacerbated cardiopulmonary injury and oxidative stress from inhaled emission particulate matter. Toxicol. Appl. Pharmacol. 164, 250–263.

Lay, J.C., Bennett, W.D., Ghio, A.J., Bromberg, P.A., Costa, D.L., Kim, C.S., Koren, H.S., Devlin, R.B., 1999. Cellular and biochemical responses of the human lung after intrapulmonary instillation of ferric oxide particles. Am. J. Respir. Cell Mol. Biol. 20, 631–642.

Lee, K.P., Trochimowicz, J.H., Reinhardt, C.F., 1985. Pulmonary response of rats exposed to titanium dioxide (TiO_2) by inhalation for two years. Toxicol. Appl. Pharmacol. 79, 179–192.

Li, N., Karin, M., 1999. Is NF-κB the sensor of oxidative stress? FASEB 13, 1137–1143.

Li, X.Y., Gilmour, P.S., Donaldson, K., MacNee, W., 1996. Free radical activity and pro-inflammatory effects of particulate air pollution (PM_{10}) in vivo and in vitro. Thorax 51, 1216–1222.

Lucesoli, F., Caligiuri, M., Roberti, M.F., Perazzo, J.C., Fraga, C.G., 1999. Dose-dependent increase of oxidative damage in the testes of rats subjected to acute iron overload. Arch. Biochem. Biophys. 372, 37–43.

Nadadur, S.S., Kodavanti, U.P., 2002. Altered gene expression profiles of rat lung in response to an emission particulate and its metal constituents. J. Toxicol. Environ. Health A 65, 1333–1350.

Peters, A., Doring, A., Wichmann, H.-E., Koenig, W., 1997. Increased plasma viscosity during an air pollution episode: a link to mortality? Lancet 349, 1582–1587.

Pope III, C.A., Dockery, D.W., Kanner, R.E., Villegas, G.M., Schwartz, J., 1999. Oxygen saturation, pulse rate, and particulate air pollution: a daily time-series panel study. Am. J. Respir. Crit. Care Med. 159, 365–172.

Pope III, C.A., Thun, M.J., Namboodiri, M.M., Dockery, D.W., Evans, J.S., Speizer, F.E., Health Jr, C.W., 1995. Particulate air pollution as a predictor of mortality in a prospective study of US adults. Am. J. Respir. Dis. Criti. Care Med. 151, 669–674.

Pritchard, R.J., Ghio, A.J., Lehmann, J.R., Winsett, D.W., Tepper, J.S., Park, P., Gilmour, M.I., Dreher, K.L., Costa, D.L., 1996. Oxidant generation and lung injury after particulate air pollutant exposure increase with the concentrations of the associated metals. Inhal. Toxicol. 8, 457–477.

Quay, J.L., Reed, W., Samet, J., Devlin, R.B., 1998. Air pollution particles induce IL-6 gene expression in human airway epithelial cells via NF-kappaB activation. Am. J. Respir. Cell Mol. Biol. 19, 98–106.

Rahman, I., 2000. Regulation of nuclear factor-κB, activator protein-1, and glutathione levels by tumor necrosis factor-κ and dexamethasone in alveolar epithelial cells. Biochem. Pharmacol. 60, 1041–1049.

Rahman, I., MacNee, W., 1999. Lung glutathione and oxidative stress: implications in cigarette smoke-induced airway disease. Am. J. Physiol. Lung Cell Mol. Physiol. 277, L1067–L1088.

Rahman, I., MacNee, W., 2000. Oxidative stress and regulation of glutathione in lung inflammation. Eur. Respir. J. 16, 534–554.

Rice, T.M., Robert, W.C., Godleski, J.J., Al-Mutairi, E., Jiang, N.-F., Hauser, R., Paulauskis, J.D., 2001. Differential ability of transition metals to indice pulmonary inflammation. Toxicol. Appl. Pharmacol. 177, 46–53.

Ritrievi, K.E., Longwell, J.P., Sarofim, A.F., 1987. The effects of ferrocene addition on soot particle inception and growth in premixed ethylene flames. Combust. Flame 70, 17–31.

Saffiotti, U., Montesano, R., Selladumar, A.R., Cefis, F., Kaufman, D.G., 1972. Respiratory tract carcinogenesis in hamsters induced by different numbers of administrations of benzo(*a*)pyrene and ferric oxide. Cancer Res. 32, 1073–1081.

Saldiva, P.H.N., Clarke, R.W., Coull, B.A., Stearns, R.C., Lawrence, J., Murthy, G.G.K., Diaz, E., Koutrakis, P., Suh, H., Tsuda, A., Godleski, J.J., 2002. Lung inflammation induced by concentrated ambient air particles is related to particle composition. J. Respir. Crit. Care Med. 165, 1610–1617.

Samet, J.M., Silbajoris, R., Huang, T., Jasper, I., 2002. Transcrioption factor activation following exposure of an intact lung preparation to metallic particulate matter. Environ. Health Perspect. 110, 985–990.

Schlesinger, R.B., 1995. Interaction of gaseous and particulate pollutants in the respiratory tract: mechanisms and modulators. Toxicology 105, 315–325.

Sharma, R., Coats, A.J.S., Anker, S.D., 2000. The role of inflammatory mediators in chronic heart failure: cytokines, nitric oxide, and endothelin-1. Int. J. Cardiol. 72, 175–186.

Shaw, G.-C., Kao, H.-S., Sung, C.-C., Chiang, A.-N., 1997. Iron and salicylate induction of cytochrome $P450_{BM-1}$ in *Bacillus megaterium*. Curr. Microbiol. 35, 28–31.

Smith, K.R., Aust, A.E., 1997. Mobilization of iron from urban particulates leads to generation of reactive oxygen species in vitro and induction of ferritin synthesis in human lung epithelial cells. Chem. Res. Toxicol. 10, 828–834.

Stokinger, H.E., 1984. A review of world literature finds iron oxides noncarcinogens. Am. Ind. Hyg. Assoc. J. 45, 127–133.

Tietz, F., 1969. Enzymatic method for quantitative determination of nanogram amounts of total and oxidized glutathione: application to mammalian blood and other tissues. Anal. Biochem. 27, 502–522.

Ulrich, M.M.W., Alink, G.M., Kumarathasan, P., Vincent, R., Boere, A.J.F., Cassee, F.R., 2002. Health effects and time course of particulate matter on the cardiopulmonary system in rats with lung inflammation. J. Toxicol. Environ. Health A 65, 1571–1595.

van Eden, S.F., Hogg, J.C., 2002. Systemic inflammatory response induced by particulate matter air pollution: the importance of bone-marrow stimulation. J. Toxicol. Environ. Health A 65, 1597–1613.

Yang, G.-S., Teague, S., Pinkerton, K., Kennedy, I., 2001. Synthesis of an ultrafine iron and soot aerosol for the evaluation of particle toxicity. Aerosol Sci. Technol. 35, 759–766.

Zhang, J., Megaridis, C.M., 1996. Soot suppression by ferrocene in laminar ethylene/air nonpremixed flames. Combust. Flame 105, 528–540.